Audio Engineering Society

Convention Paper

Presented at the 112th Convention
2002 May 10–13 Munich, Germany

Suspension Bounce as a Distortion Mechanism in Loudspeakers with a Progressive Stiffness

D. B. (Don) Keele Jr.[1] and Ryan J. Mihelich[1]
E-mail: DKeele@Harman.com, RMihelic@Harman.com

[1]*Harman/Becker Automotive Systems, Martinsville, IN 46151, U.S.A*

ABSTRACT

The stiffness of a progressive suspension is fairly constant for small excursions and then gets progressively stiffer for larger excursions. When the moving assembly enters the region of increasing stiffness, forces are generated that rapidly reverse its motion much the same as when a bouncing ball hits the ground. Contrary to the common wisdom that predicts a squared-off displacement waveform, the bouncing-ball analogy predicts that the displacement waveform will be turned into a triangle wave. Under some conditions, the moving assembly will repetitively bounce at a frequency tens of times higher than the excitation frequency with acoustic output that exhibits high-level harmonics several times higher in amplitude and frequency than the fundamental. Time-domain simulations and experiments are presented to illustrate the effects.

0 INTRODUCTION

Loudspeaker suspensions are nonlinear devices that often exhibit a fairly constant stiffness over some excursion range and then get progressively stiffer as the diaphragm moves beyond this range. At high drive levels, this characteristic causes problems in the motion of the diaphragm much akin to the dynamics and forces experienced by a bouncing ball. When the moving assembly enters the region of increasing stiffness, high forces are generated that rapidly reverse its motion.

Under these conditions, common wisdom predicts that the displacement of the driver gets squared off creating a form of distorted square wave. Contrary to this prediction, the bouncing-ball analogy predicts that the peaks of the displacement waveform will be sharpened and the whole waveform will be turned into a triangle wave.

Under certain circumstances, when the outward motor Bli force exceeds the restoring force of the suspension in its linear range, the moving assembly will repetitively bounce off the region of increasing stiffness. This bounce frequency may be tens of times higher than the excitation frequency. The resultant acoustic output will be extremely distorted and exhibit high-level harmonics several times higher than the fundamental both in level and frequency.

Although several authors have analyzed the effects of non-linear suspension compliance [1 – 5], none have pointed out the bouncing-like phenomenon that occurs when the excursion approaches and exceeds the limits of a progressive suspension.

A time-domain simulation is used to provide an analysis of a progressive suspension, showing its effects on low frequency

distortion versus drive level and frequency. Experimental measurements on several drivers confirm the bounce effects.

1 THEORY

1.1 Bouncing Ball Analogy

The physics of the bouncing ball is an apt analogy to what happens to the moving system of a loudspeaker when it interacts with the progressive stiffness of the loudspeaker suspension. When the excursion of the diaphragm enters the region of high suspension stiffness, the suspension pushes back with much higher force. This is analogous to the forces presented to a bouncing ball when it makes contact with the ground.

When the ball is in the air, the only force on the ball is due to gravity, which accelerates it towards the ground. When it contacts the ground, a high upwards force much exceeding the downward force of gravity is experienced by the ball due to the ball's internal stiffness. This very-high upward force causes the ball to rapidly reverse direction and head upwards. At each bounce, some energy is lost when the ball is in contact with the ground. This causes each successive bounce to rebound to a lower height than the previous. The very-high effective stiffness of the ball generates very-high forces when it contacts the ground. This minimizes ground contact time.

1.2 Bouncing Ball Simulation

A model was created to compute the instantaneous time values of the motion of a bouncing ball. The following set of first-order differential equations model the dynamics of the ball.

$$\text{Velocity} = v = \frac{dh}{dt}$$

$$\text{Acceleration} = \frac{dv}{dt} = \text{force/mass} = \begin{cases} -G & \text{for } h > 0 \\ (-K_B x - R_B v)/M_B & \text{for } h \le 0 \end{cases} \quad (1)$$

Where h = height (m)

G = acceleration of gravity (9.8 m/s^2)

K_B = ball compression stiffness (N/m)

R_B = ball mechanical loss in ohms (N/m/s)

M_B = ball mass (kg)

These coupled first-order differential equations were solved numerically using a general ODE (ordinary differential equation) solver in a general-purpose math program.

Figure 1 illustrates the results of a simulation using this simple bouncing-ball model. The graph shows plots of the ball's instantaneous displacement, velocity, acceleration, and force as a function of time for a ball that is dropped from a fixed initial height of 2 meters. The model neglects air resistance but does include mechanical losses when the ball is in contact with the ground. The simulation used the following parameters: M_B = 0.5 kg, K_B = 10,000 N/m, R_B = 10 mechanical ohms, and a simulation time of 3 seconds.

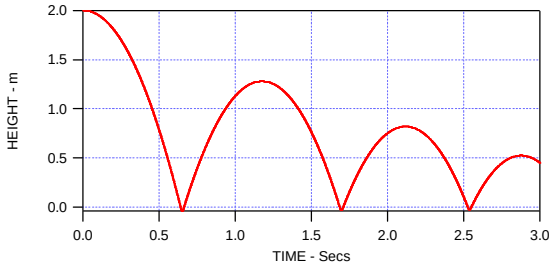

Fig. 1a. Plot of displacement versus time for a ball dropped from an initial height of 2 m. The ball has a mass of 0.5 kg, a compression stiffness of 10,000 N/m, and a compression mechanical loss of 10 N/m/sec.

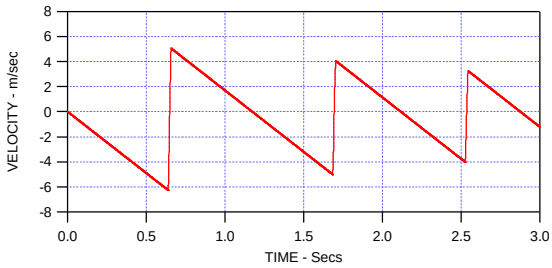

Fig. 1b. Velocity versus time for bouncing ball.

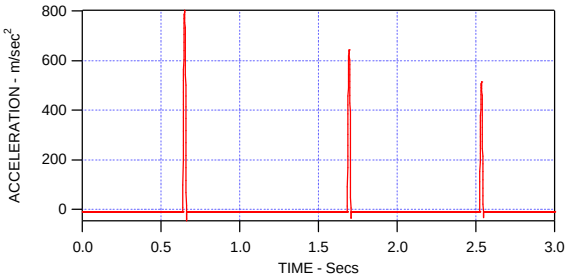

Fig. 1c. Acceleration versus time for bouncing ball.

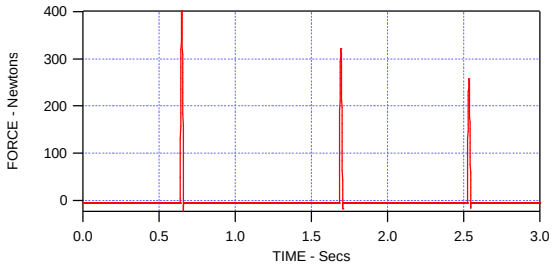

Fig. 1d. Force on bouncing ball versus time.

Figure 1 tracks the ball for 3 bounces. The displacement (a) shows the typical bouncing ball time signature with each successive bounce rising to a smaller height than the previous one due to ground-contact damping losses. The velocity Fig. 1(b) shows the linear decreasing velocity while the ball is in the air interspersed with sudden shifts in velocity from negative to positive while in contact with the ground.

The acceleration Fig.1(c) shows the constant –9.8 m/sec downward acceleration of gravity when the ball is in the air, interspersed with sharp high-amplitude upward positive spikes of acceleration when the ball contacts the ground. The ball contacts

the ground for only about 20 ms on each bounce. The short high-amplitude acceleration spikes are a result of the very-high momentary upward forces the ball experiences when in ground contact Fig. 1(d).

The short high-amplitude spikes in the force and acceleration versus time graphs are a typical of bouncing. As will be shown later, this characteristic is an identifying phenomenon of suspension bounce in loudspeakers.

1.3 Loudspeaker Motion

The constant stiffness of a perfectly linear loudspeaker suspension provides a restoring force directly proportional and opposite in sign to the speaker's displacement from its rest position.

In a loudspeaker with a progressive suspension, the stiffness is somewhat constant over a certain displacement range but then increases suddenly for displacements beyond this point. When the moving (diaphragm) assembly enters an excursion region of rapidly-increasing stiffness, the suspension pushes back with much more force than it would have otherwise.

The current flowing in the voice coil of the loudspeaker provides the primary force (Bli) driving the moving assembly outward. The restoring force of the suspension acts in opposition to this outward movement. The resultant direction of movement depends on the relative strengths of each of these forces and the mass reaction forces due to the cone's motion. The interplay of these forces and their effects on the dynamics of the moving system of the loudspeaker is the topic of this paper.

2 SIMULATIONS

Loudspeakers were simulated with various degrees of suspension nonlinearity, using a sine wave drive of various levels, and frequency. All simulated drivers included only a non-linear suspension, all other driver parameters were linear. All simulations assume low-frequency behavior where all the electrical, mechanical, and acoustical parameters of the loudspeaker can be considered as lumped elements.

2.1 Simulator Description

As before, with the bouncing ball model, a simulator using a general ODE solver from a general-purpose math program was used to solve the coupled set of first-order differential equations describing the loudspeaker driver.

2.2 Nonlinear Loudspeaker Model

The modeled loudspeaker contains only a non-linear suspension, i.e. a compliance that is a function of the voice-coil position. Voice coil inductance was neglected as well as acoustic radiation. The loudspeaker was assumed to be mounted in an infinite baffle.

The following set of coupled first-order differential equations describe the loudspeaker:

$$\text{Velocity} = v = \frac{dx}{dt}$$

$$\text{Acceleration} = \frac{dv}{dt} = \text{force/mass} = \frac{\left[Bl\dfrac{(V_{in} - Blv)}{R_E} - \dfrac{x}{C_{MS}(x)} - R_{MS}v \right]}{M_{MS}} \qquad (2)$$

Where $x =$ excursion (m)

$M_{MS} =$ driver moving mass (kg)

$C_{MS}(x) =$ non-linear suspension compliance (m/N), assumed to be a function of the instantaneous displacement x

$R_{MS} =$ mechanical loss of suspension (N/m/s)

$R_E =$ voice-coil resistance (Ohms)

$B =$ magnetic flux density (T)

$l =$ length of voice-coil conductor (m)

$V_{in} =$ input voltage (V)

2.3 Nonlinear Suspension Models

The only non-linearity modeled in this loudspeaker simulation is the suspension compliance, which is a function of the voice-coil's instantaneous displacement x. Two symmetrical non-linear compliance models were defined in this simulation: 1. a model that simulates progressive suspensions based on a Butterworth magnitude function which has a linear region for small excursions and a rapid compliance drop off for higher excursions, and 2. a Gaussian-function based model that loosely simulates some real-world compliance non-linearity's that are typically more rounded and less progressive.

2.3.1 Butterworth Model

A progressive symmetrical dependence of compliance on excursion is modeled by the following function. It models a compliance that is somewhat linear for excursions less than a certain value, and then rapidly decreases for larger excursions. A parameter is included that defines the degree of progressiveness. A more progressive compliance is linear over a wider range and then falls off more rapidly. This function is based on the Butterworth magnitude functions for band-pass filters. The function appears as:

$$C_{MS}(x) = \frac{C_0}{\sqrt{\sqrt{1+|x|^n}}} = \frac{C_0}{(1+|x|^n)^{0.25}} \qquad (3)$$

Where $x =$ normalized excursion, $\dfrac{x}{x_{\max}}$

$C_0 =$ rest position compliance, $C_{MS}(0)$

$n =$ progressiveness parameter,
i.e., $n < 4$ low progressiveness,
$n > 10$ high progressiveness.

Figure 2 shows plots of this function for various values of the progressiveness parameter n.

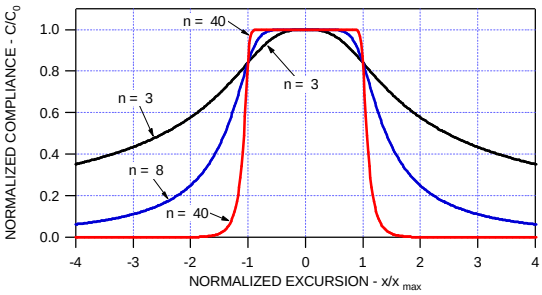

Fig. 2. Plot of the symmetrical Butterworth compliance model for various values of the progressiveness parameter n = (3, 8, 40). Higher values provide higher progressiveness.

2.3.2 *Gaussian Model*

A rounded bell-curve-like symmetrical compliance dependence on excursion is modeled by the following equation:

$$C_{MS}(x) = C_0 e^{-C_1 x^2} \qquad (4)$$

Where x = normalized excursion, $\frac{x}{x_{max}}$

C_0 = rest position compliance, $C_{MS}(0)$

C_1 = a constant that defines the width of the curve, i.e. $C_1 < 1$ wide, $C_1 > 1$ narrow.

Figure 3 shows plots of this function for various values of the width parameter.

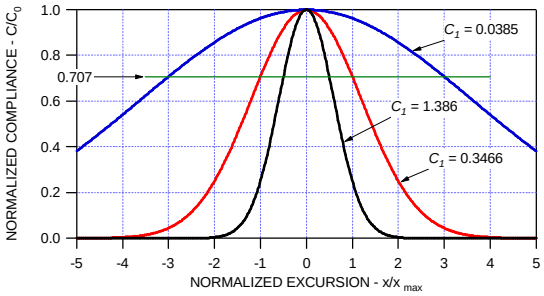

Fig. 3. Plot of the symmetrical Gaussian compliance model for various values of the width parameter C_1 = (0.0385, 0.3466, 1.3866). These values provide widths of 6, 2, and 1 respectively at the 0.707 normalized compliance level. Higher values yield smaller widths.

2.4 Simulation Results

Using the simulator described previously in sections 2.1 and 2.2 and the driver parameters given in Table 1, a loudspeaker was simulated under different conditions. The effects of varying frequency, amplitude, suspension characteristic, and mechanical damping are studied.

Table 1: LOUDSPEAKER MECHANICAL DRIVER PARAMETERS

Parameter	Value
Moving Mass, M_{MS}	0.063 kg
Suspension Compliance, C_{MS}	0.00017 m/N
Bl Factor	5.0 N/A
Mechanical Resistance of Suspension, R_{MS}	0.0 Mechanical Ohms
Voice-coil DC Resistance, R_E	6.6 Ohms
Peak Displacement, X_{max}	0.002 m
Free-air Resonance Frequency, f_S	48.6 Hz

2.4.1 *Frequency Dependence Holding Excursion Constant with a Highly-Progressive Suspension*

The effect of changing the electrical input frequency is illustrated here by holding the peak excursion of the loudspeaker constant and varying the sinusoidal input frequency. Plots of driver instantaneous excursion are shown for frequencies of 1, 5, 10, 20, and 35 Hz. The input voltage was varied to maintain a constant normalized excursion of roughly ±1.2 and varied from 14 Vrms at low frequencies down to 5 Vrms at higher frequencies.

For this experiment, the highly progressive Butterworth nonlinear suspension characteristic described by Eq. 3 with n = 40 was used and is shown in Fig. 4. This peak-to-peak excursion value encroaches heavily into the progressive suspension region and reduces the compliance to 30% of its maximum value.

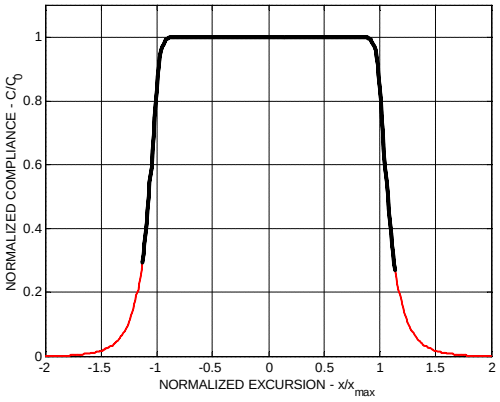

Fig. 4. Plot of the normalized compliance versus the normalized excursion for n = 40. This high value of n provides a highly progressive suspension. The thick black line indicates the excursion range that the driver experienced during the simulations shown in the following five figures (Figs. 5 – 9). The asymmetry of the thick black line is due to the startup transient.

The figures illustrate the full range of suspension bounce exhibited by a loudspeaker. Note that the simulation starts at t = 0 with a suddenly applied sinewave and includes the free response of the somewhat electro-magnetically under-damped loudspeaker.

The frequency range can be divided roughly into four separate regions:
1. Very-low frequencies where the suspension bounce is minimal and the excursion waveform is squared off (Fig. 5),
2. Low frequencies where the repetitive nature of suspension bounce is most evident (Figs. 6-7),
3. Frequencies just below resonance where suspension bounce turns the excursion waveform into a sharp-cornered triangular like wave (Figs. 8-9), and
4. High frequencies above resonance where the excursion is significantly below the progressive excursion limit at normal operating levels and a clean waveform is produced (Fig. not shown).

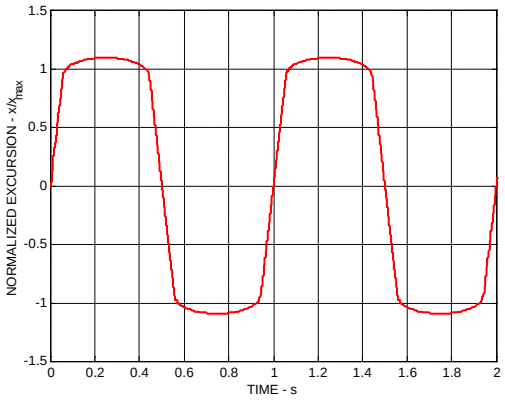

Fig.5. Excursion versus time at 1 Hz for the loudspeaker of Table 1. The highly-progressive suspension of Fig. 4 was used with an input drive of 14 Vrms. Note the rounded upper and lower peaks of the waveform that occur at this low frequency.

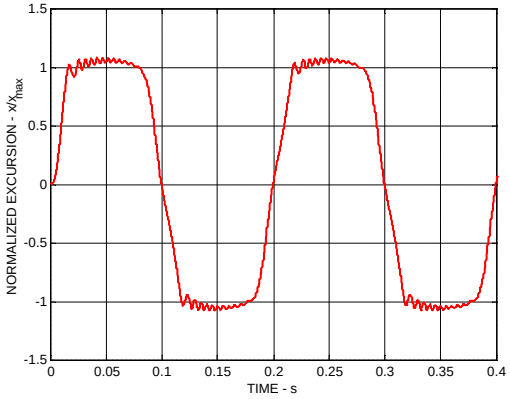

Fig. 6. Excursion versus time at 5 Hz for the loudspeaker of Table 1. The highly progressive suspension of Fig. 4 was used with an input drive of 14 Vrms. Note the start of suspension bounce, which is indicated by the ringing in the waveform.

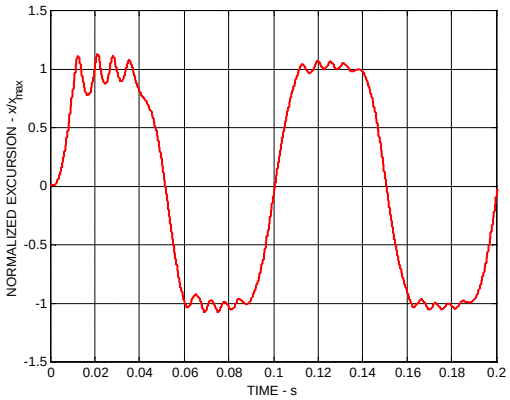

Fig. 7. Excursion versus time at 10 Hz for the loudspeaker of Table 1. The highly progressive suspension of Fig. 4 was used with an input drive of 8 Vrms. Note the higher amplitude suspension bounce. The bouncing appears to occur at a lower rate only because the timescale of the graph has changed.

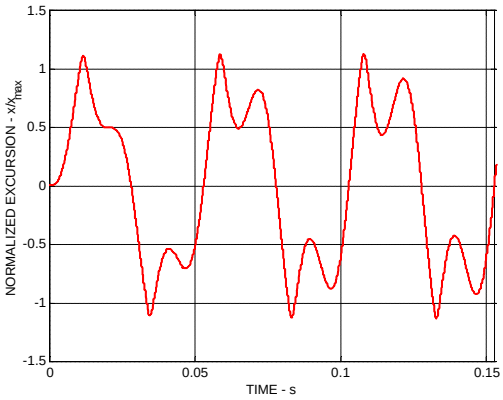

Fig. 8. Excursion versus time at 20 Hz for the loudspeaker of Table 1. The highly progressive suspension of Fig. 4 was used with an input drive of 5 Vrms. Four cycles of suspension bounce occur for roughly each cycle of the fundamental.

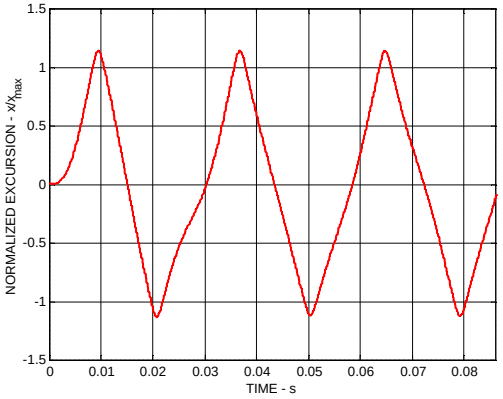

Fig. 9. Excursion versus time at 35 Hz for the loudspeaker of Table 1. The highly progressive suspension of Fig. 4 was used with an input drive of 5 Vrms. At this frequency, the excursion waveform has turned into a triangular wave. The diaphragm only bounces twice per input cycle.

2.4.2 Amplitude Dependence with a Highly-progressive Suspension

The effect of changing the input electrical amplitude is illustrated in the following six graphs (Figs. 10 – 15).. A linear amplitude-modulated sine wave 10-cycle up-down ramp signal was used to energize the loudspeaker. The input signal is shown in Fig. 10.

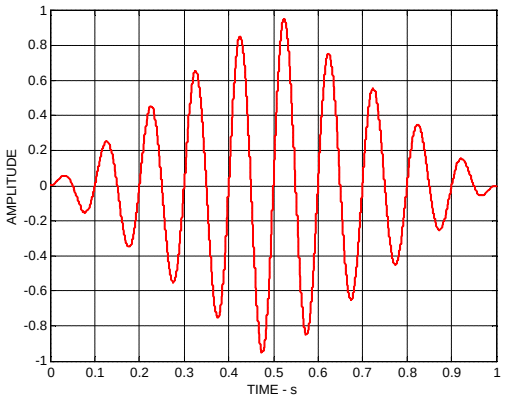

Fig. 10. Up-down ramp sine wave electrical input signal used to investigate the amplitude dependence of the suspension non-linearity. The signal is a 10-cycle amplitude-modulated sinewave burst with a linear 5-cycle up ramp followed by a linear 5-cycle down ramp.

In addition to a plot of excursion at each frequency, additional graphs of velocity and acceleration have been added. Note that the acoustic output of the loudspeaker is proportional to the cone's acceleration. As before, graphs are shown for frequencies of 1, 5, 10, 20, and 35 Hz (Figs. 11 – 15). A maximum input level of 20 Vrms (28.28 Vpeak) was used for all simulations except for the 35 Hz simulation (Fig. 15) where the maximum level was reduced to 14 Vrms (19.8 Vpeak).

The 1-Hz data is shown in Fig. 11. Here the excursion waveform is essentially squared (rounded) off and shows none of the visible effects of suspension bounce. However, the velocity and acceleration plots clearly show the beginning effects of bouncing in the rapid much-higher frequency oscillations that appear. The acceleration (hence acoustic output) plot essentially consists of only bouncing effects.

At higher frequencies, the bouncing appears quite strongly in the excursion waveform, and also very strongly in the velocity and acceleration waveforms. At the lower frequencies, the bouncing frequency is significantly higher than the test frequency and appears as hash on the waveforms. At 20 Hz (Fig. 14), the bounce frequency is only somewhat higher than the test frequency, so that individual cycles of the bouncing can be clearly seen. Note the individual spikes in the acceleration waveform at a drive frequency of 35 Hz (Fig. 15), which mimic the characteristic acceleration spikes in the bouncing ball simulation of Fig. 1c.

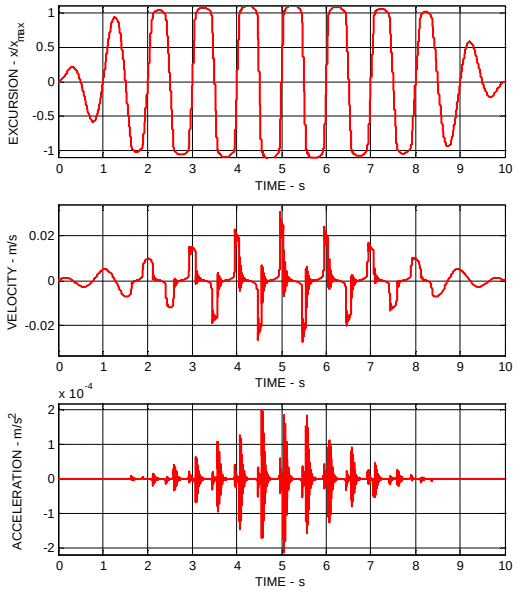

Fig. 11. Excursion (top), velocity (middle) and acceleration (bottom) at 1 Hz for the loudspeaker of Table 1. The highly progressive suspension of Fig. 4 was used with the drive signal shown in Fig. 10 with maximum amplitude of 20 Vrms (28.28 Vpeak). Note that while excursion reaches a maximum quickly, acceleration (which is proportional to sound pressure) increases continuously over the time range of increasing input voltage.

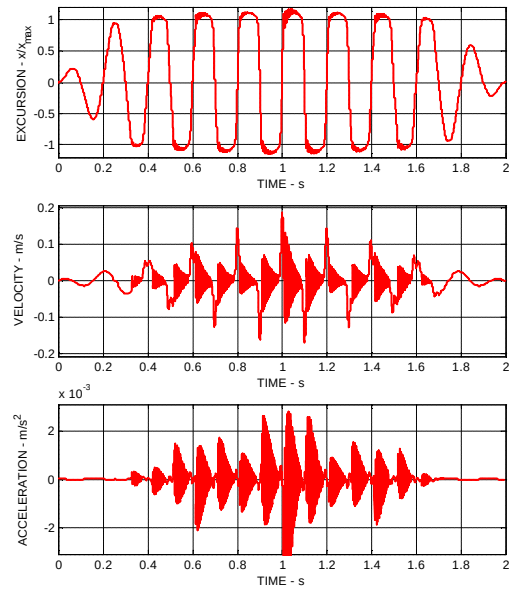

Fig. 12. Excursion (top), velocity (middle) and acceleration (bottom) at 5 Hz for the loudspeaker of Table 1. The highly progressive suspension of Fig. 4 was used with the drive signal shown in Fig. 10 with maximum amplitude of 20 Vrms (28.28 Vpeak).

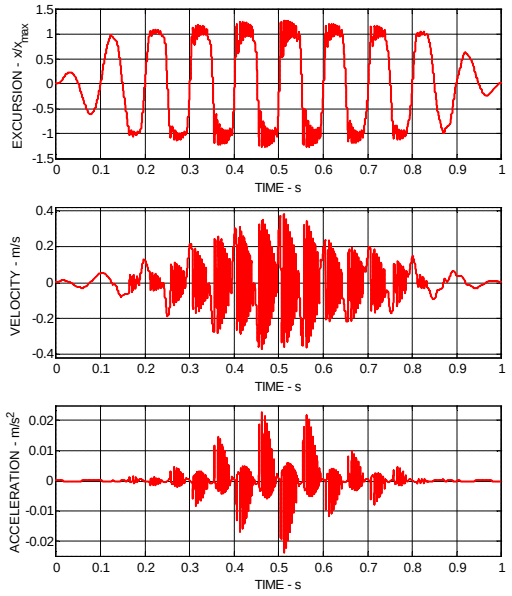

Fig. 13. Excursion (top), velocity (middle) and acceleration (bottom) at 10 Hz for the loudspeaker of Table 1. The highly progressive suspension of Fig. 4 was used with the drive signal shown in Fig. 10 with maximum amplitude of 20 Vrms (28.28 Vpeak).

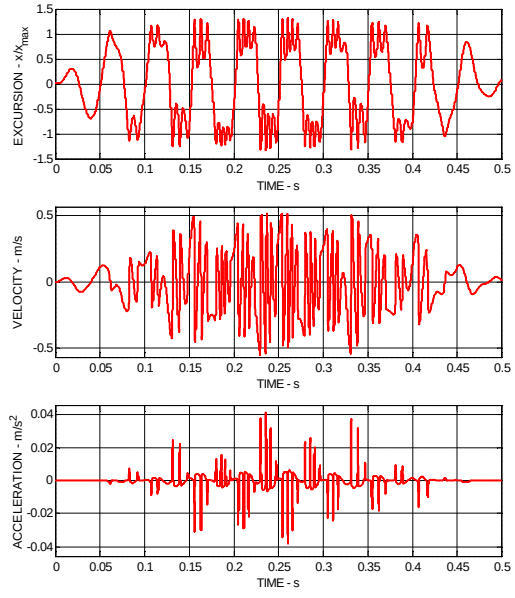

Fig. 14. Excursion (top), velocity (middle) and acceleration (bottom) at 20Hz for the loudspeaker of Table 1. The highly progressive suspension of Fig. 4 was used with the drive signal shown in Fig. 10 with maximum amplitude of 20 Vrms (28.28 Vpeak).

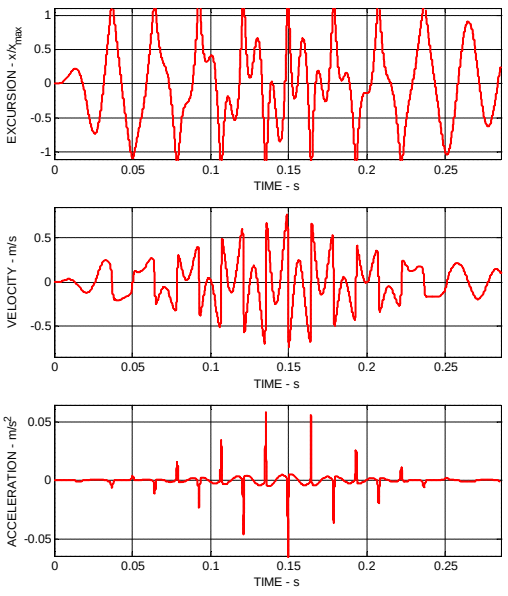

Fig. 15. Excursion (top), velocity (middle) and acceleration (bottom) at 35Hz for the loudspeaker of Table 1. The highly progressive suspension of Fig. 4 was used with the drive signal shown in Fig. 10 with maximum amplitude of 14 Vrms (19.8 Vpeak).

2.4.3 *Amplitude Dependence with a Less-Progressive Suspension*

The behavior shown in the previous sections using the strongly progressive (n = 40) Butterworth model is considered extreme but it is shown to exemplify the effects that are observable in more realistic cases. The Gaussian suspension model is more realistic of typical suspensions because of its more rounded-off character and absence of steep compliance drop offs at extreme values of excursion. The Gaussian suspension model used for the following simulations is shown in Fig. 16.

The following graphs repeat the same test sequence of the previous section with the 10-cycle up-down ramped sinewave, but with the Gaussian suspension model. As before, trios of excursion-velocity-acceleration graphs are shown for frequencies of 1, 5, 10, 20, and 35 Hz (Figs. 17 – 21). Also as before, a maximum input level of 20 Vrms (28.28 Vpeak) was used for all simulations except for the 35 Hz simulation (Fig. 21) where the maximum level was reduced to 14 Vrms (19.8 Vpeak). The maximum excursion reached in these simulations rose to twice x_{max}, which reduced the compliance to about 0.25 of its resting (x = 0) value.

Although this suspension model is much more gentle as compared to the highly progressive model (Fig. 4) used in the previous sections, these graphs still exhibit strong bounce effects.

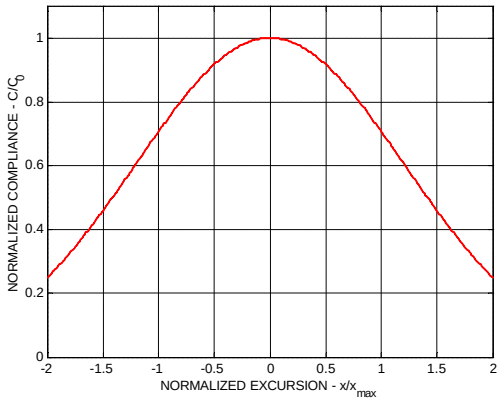

Fig. 16. Plot of the normalized compliance versus the normalized excursion for C_1=0.3466. This value of C_1 provides a compliance which diminishes to 70.7% of its x=0 value at a normalized excursion of 1.

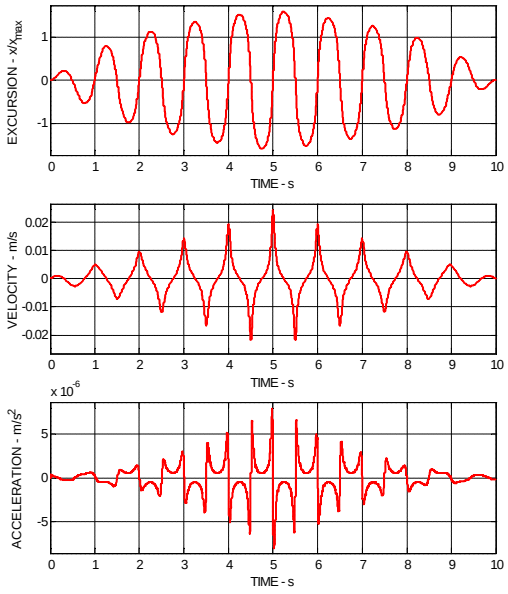

Fig. 17. Excursion (top), velocity (middle) and acceleration (bottom) at 1 Hz for the loudspeaker of Table 1. The less-progressive Gaussian suspension of Fig. 16 was used with an input drive which ramps from 0 Vrms to 20 Vrms linearly over 5 cycles, then back to 0 Vrms over the next 5 cycles.

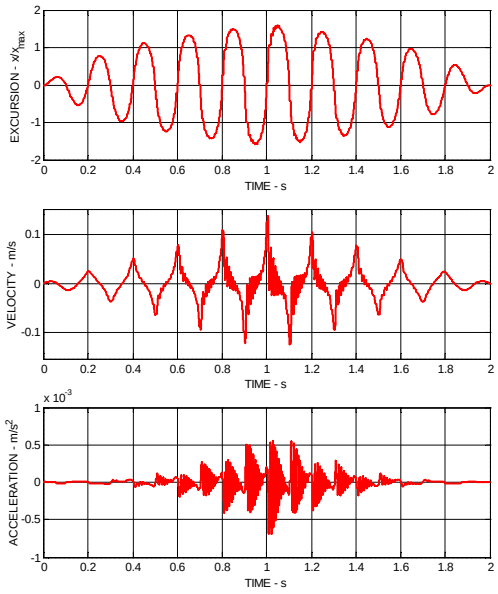

Fig. 18. Excursion (top), velocity (middle) and acceleration (bottom) at 5Hz for the loudspeaker of Table 1. The less-progressive Gaussian suspension of Fig. 16 was used with the drive signal shown in Fig. 10 with maximum amplitude of 20 Vrms (28.28 Vpeak).

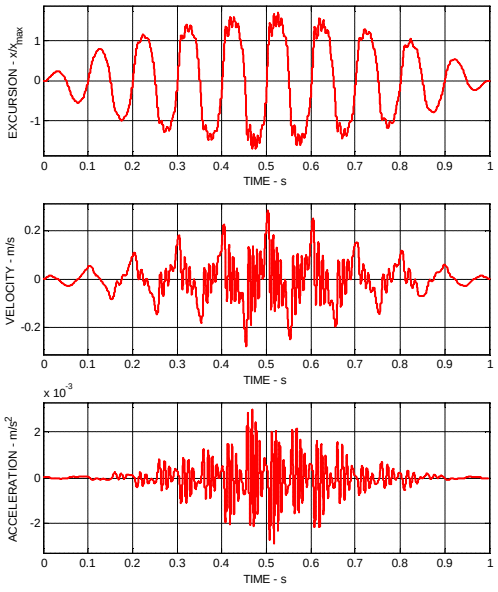

Fig. 19. Excursion (top), velocity (middle) and acceleration (bottom) at 10Hz for the loudspeaker of Table 1. The less-progressive Gaussian suspension of Fig. 16 was used with the drive signal shown in Fig. 10 with maximum amplitude of 20 Vrms (28.28 Vpeak).

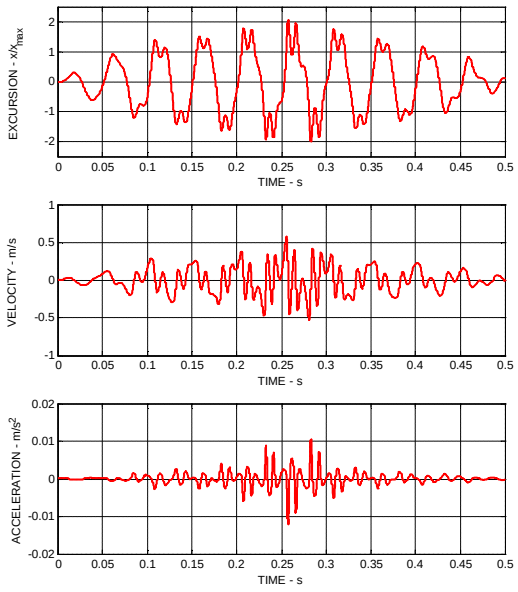

Fig. 20. Excursion (top), velocity (middle) and acceleration (bottom) at 20Hz for the loudspeaker of Table 1. The less-progressive Gaussian suspension of Fig. 16 was used with the drive signal shown in Fig. 10 with maximum amplitude of 20 Vrms (28.28 Vpeak).

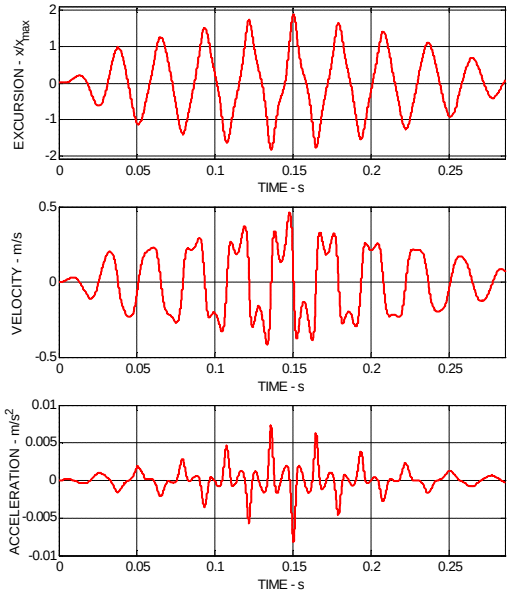

Fig. 21. Excursion (top), velocity (middle) and acceleration (bottom) at 35Hz for the loudspeaker of Table 1. The less-progressive Gaussian suspension of Fig. 16 was used with the drive signal shown in Fig. 10 with maximum amplitude of 14 Vrms (19.8 Vpeak).

2.4.4 Effect of Suspension Damping

The following two figures illustrate the effect of suspension damping on the bounce phenomena with a highly progressive suspension. The un-damped 10-Hz-data of a previous simulation (Fig. 13) was used as a base line. Note that the vertical scales of the two following graphs match that of Fig. 13.

The data in Fig. 22 shows the effect of raising the suspension's mechanical resistance R_{ME} from zero (no damping) to 10 mechanical ohms. This amount of added loss caused a significant reduction in the bouncing without causing any loss of amplitude at input levels below that which triggers bouncing.

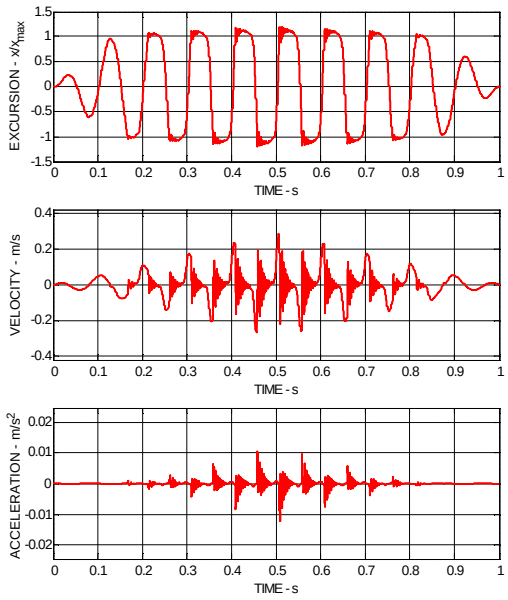

Fig. 22. Excursion (top), velocity (middle) and acceleration (bottom) at 10 Hz for the loudspeaker of Table 1 with the mechanical loss increased from zero to 10. The highly progressive suspension of Fig. 4 was used with the up-down amplitude sine wave drive signal shown in Fig. 10 with maximum amplitude of 20 Vrms (28.28 Vpeak). Note the reduction in bouncing as compared to the no-loss situation shown in Fig. 13.

The waveforms shown in Fig. 23 illustrates the effect of a much higher amount of loss (R_{ME} = 200). Here the bounce has been essentially eliminated. Note however that this high amount of loss has significantly reduced the amplitude at input levels below those that trigger bouncing.

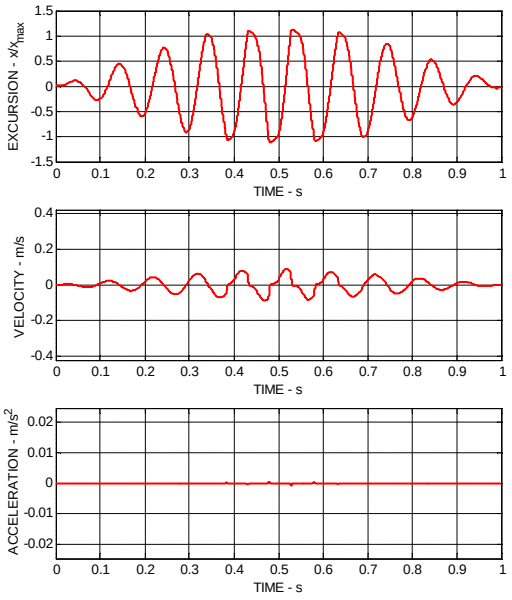

Fig. 23. Excursion (top), velocity (middle) and acceleration (bottom) at 10 Hz for the loudspeaker of Table 1 with the mechanical loss increased to the very-high level of 200. The highly progressive suspension of Fig. 4 was used with the up-down amplitude sine wave drive signal shown in Fig. 10 with a maximum amplitude of 20 Vrms (28.28 Vpeak). Note that the bouncing has essentially been eliminated from all three of the waveforms as compared to the no-loss situation shown in Fig. 13, but that the lower level amplitude signals have been significantly reduced as well due to the high damping.

2.4.5 *Distortion Spectra of Acoustic Output*

The following five figures (Figs. 24 – 28) illustrate the effect of increasing drive level on the harmonic distortion for a fixed frequency of 10 Hz with a highly progressive suspension. Input levels of 4, 8, 12, 16, and 20 Vrms are graphed. Each figure contains two graphs: in (a) the suspension's compliance versus excursion is shown with a bold line indicating the excursion range, in (b) the resulting FFT spectrum of the acceleration waveform which is proportional to the radiated acoustic output. All FFT spectrums are normalized so that the fundamental is at 0 dB.

Although graphs of excursion, velocity, and acceleration are not shown for each of the input levels, the graphs for an input level of 8 Vrms are shown in Fig. 7. All conditions except drive level are the same as the conditions for Fig. 7.

Note that rapid increase in harmonic levels due to bouncing as the excursion rises into the progressive region where the compliance is falling. Because this nonlinear compliance is perfectly symmetric, no even order harmonics are present in the spectra. At high amplitudes, the harmonics very much exceed the fundamental both in amplitude and frequency. At a drive level of 20 Vrms at 10 Hz, the twenty-fifth harmonic exceeds the fundamental by 20 dB!

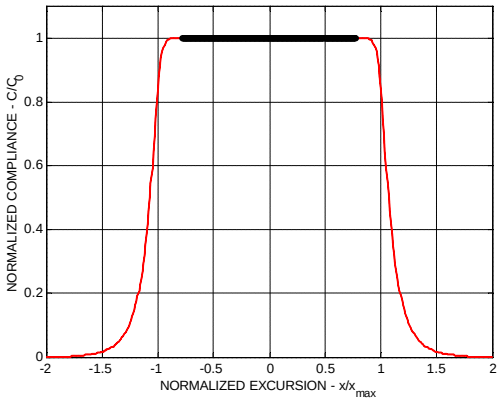

Fig. 24a. Excursion range (bold line) for a sine wave drive level of 4 Vrms at 10 Hz overlaid on the compliance versus excursion plot. This value of input allows the driver to operate entirely in the linear range of the suspension.

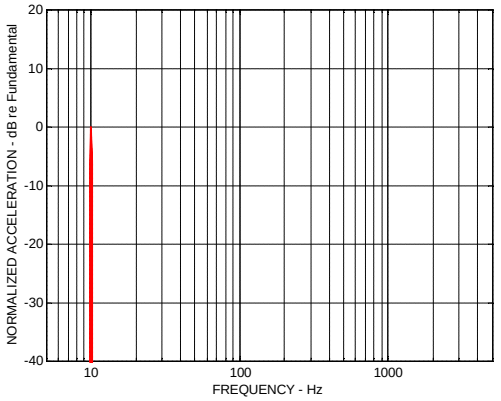

Fig. 24b. Spectrum of acoustic output (acceleration) for a 4 Vrms input at 10 Hz. At this input level only the fundamental is evident because the loudspeaker is operating in a perfectly linear region. Harmonics are not present.

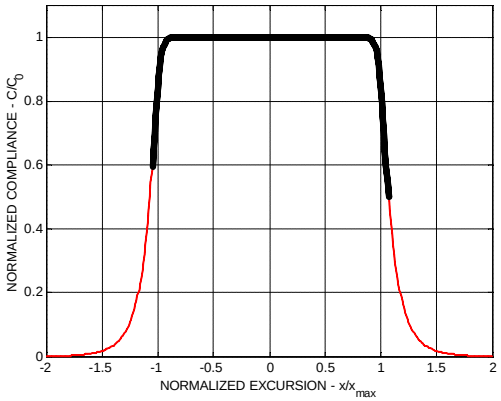

Fig. 25a. Excursion range (bold line) for a drive level of 8 Vrms at 10 Hz overlaid on the compliance versus excursion plot. Asymmetry in bold line due to startup transient.

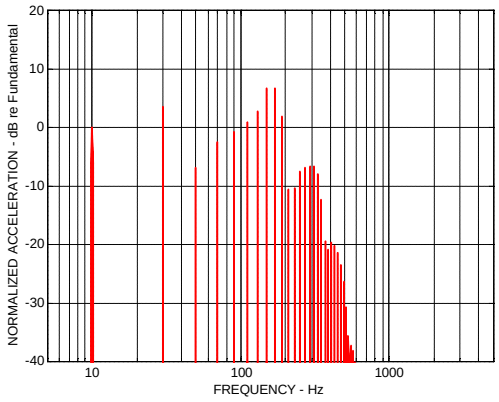

Fig. 25b. Spectrum of acoustic output (acceleration) for an 8 Vrms input at 10 Hz.

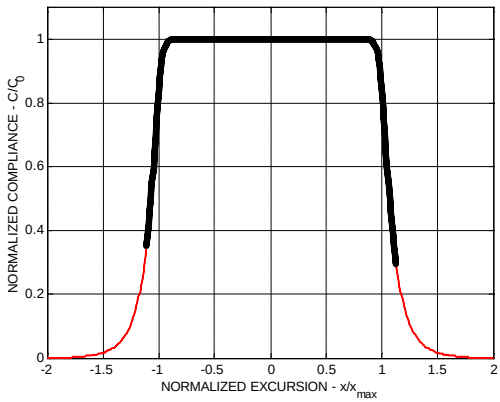

Fig 26a. Excursion range (bold line) for a drive level of 12 Vrms at 10 Hz overlaid on the compliance versus excursion plot.

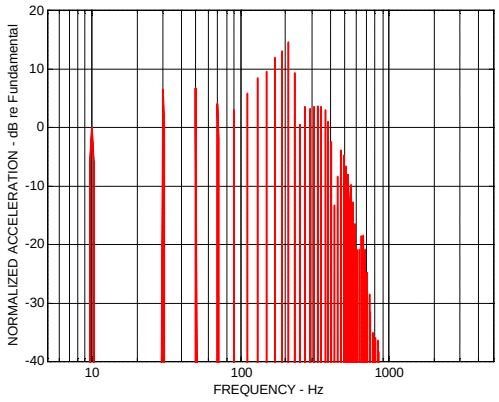

Fig 26b. Spectrum of acoustic output (acceleration) for a 12 Vrms input at 10 Hz.

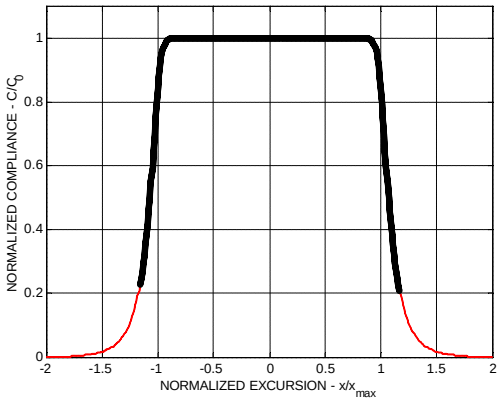

Fig. 27a. Excursion range (bold line) for a drive level of 16 Vrms at 10 Hz overlaid on the compliance versus excursion plot.

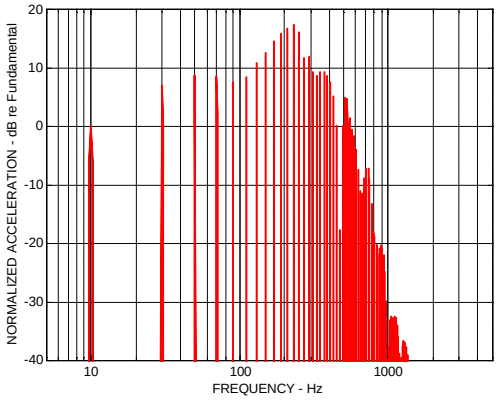

Fig. 27b. Spectrum of acoustic output (acceleration) for a 16 Vrms input at 10 Hz.

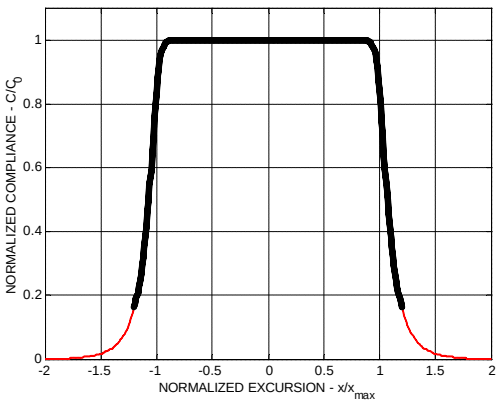

Fig. 28a Excursion range (bold line) for a drive level of 20 Vrms at 10 Hz overlaid on the compliance versus excursion plot.

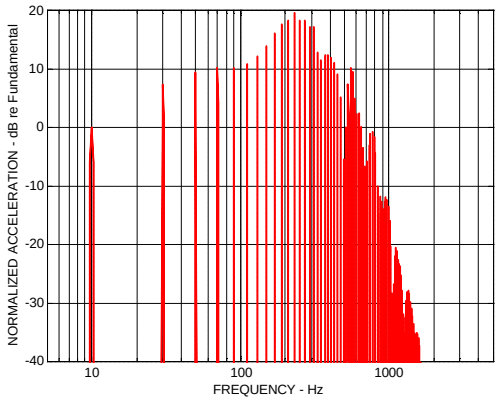

Fig. 28b. Spectrum of acoustic output (acceleration) for a 20 Vrms input at 10 Hz. The bounce effects cause the harmonics to exceed the fundamental both in level and frequency.

3 MEASUREMENTS

3.1 Measurement Setup

To show the effects of suspension bounce on an actual loudspeaker, a simple measurement setup was used consisting of a displacement laser and a digital storage oscilloscope. Time domain records of the cone excursion were recorded at several frequencies with amplitude sufficient to move the diaphragm to a region of high suspension stiffness. This amplitude was high enough to show the effect but low enough to prevent mechanical bottoming or the voice coil from burning.

3.2 Loudspeaker Measured

The loudspeaker used for these measurements is a 16cm woofer with a fairly linear and symmetric Bl versus excursion over the range –5mm to +5mm and an asymmetric, nonlinear suspension shown in Figure 29. The asymmetry in the compliance versus excursion curve causes the displacement waveforms to exhibit different behavior in the positive excursion direction than in the negative direction. The effect of the more rapid stiffening in the positive excursion direction is to cause a reduction in positive excursion as well as a different number of cycles of suspension bounce at certain frequencies. In the negative excursion direction, a higher excursion is seen with bouncing that occurs at higher amplitudes.

3.3 Measurement Description

The loudspeaker was measured at frequencies of 1, 5, 15, 25 and 50 Hz while being energized by sine waves in increasing amplitude steps. At each frequency measured, four amplitude levels are shown, each representing a 3dB increase in input voltage. At 1 Hz, only three amplitudes are shown because of thermal limitations of the loudspeaker used.

3.4 Measurement Results

The following figures show the results of the measurements.

3.4.1 Measured Compliance vs. Excursion

Fig. 29 shows the measured compliance of the test speaker versus voice-coil excursion. The compliance data was measured dynamically using a tension/compression load frame as described in [7]. Note the somewhat rounded character of the compliance curve with a roughly linear compliance between –2 to +5 mm, and a rapid roll-off for positive excursions and a less rapid roll-off for negative excursions.

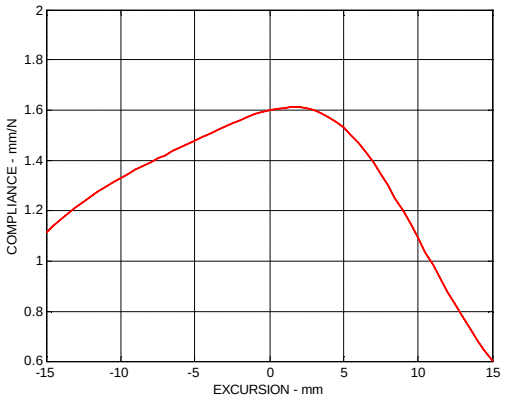

Fig. 29. Compliance versus excursion for the speaker used for measurements. The highly asymmetric nature of this curve causes the displacement waveforms to show asymmetry as well.

3.4.2 Excursion vs. Time with Sinewave Drive

The following graphs show the results of the steady-state sinewave tests at frequencies of 1, 5, 15, 25 and 50 Hz. Each graph displays three or four overlaid curves of the excursion at increasing drive levels in 3-dB steps. Time scale start times are arbitrary but time scaling is correct. Note that the vertical scale of each graph was changed to best display the data. Each graph exhibits some noise due to the laser excursion measuring apparatus. Refer to the figure captions for more information about each graph.

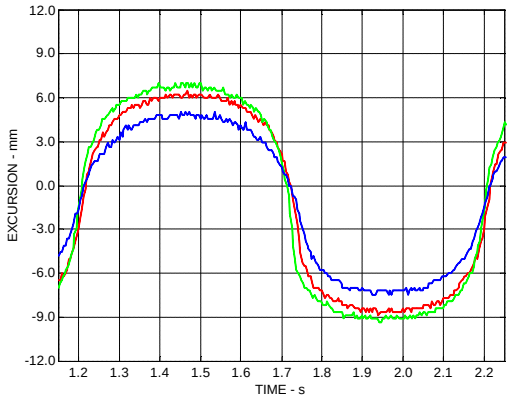

Fig. 30. Measured excursion versus time at 1 Hz. The electrical input signal was increased in 3dB steps. Notice the asymmetry about the zero-excursion axis due to the asymmetric compliance of the suspension. At this low frequency, except for a noisy waveform, no bouncing is evident.

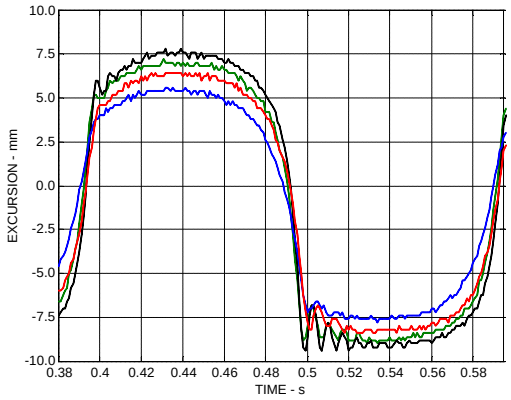

Fig. 31. Measured excursion versus time at 5 Hz. The electrical input signal was increased in 3dB steps. Note the asymmetry about the zero-excursion axis due to the asymmetric compliance of the suspension. Note also the differences in the suspension bounce between the positive and negative excursions where only a single bounce is present in the positive direction, but many cycles of bounce are present in the negative direction.

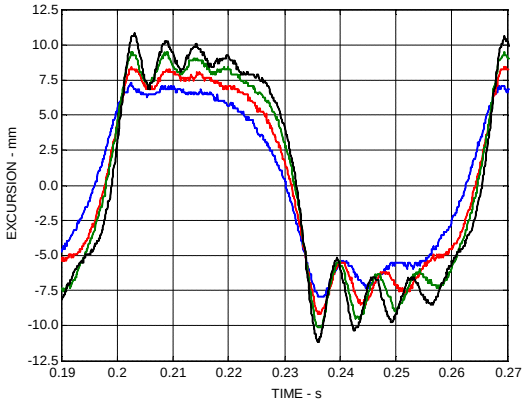

Fig. 32. Measured excursion versus time at 15 Hz. The electrical input signal was increased in 3dB steps. Note the differences in the suspension bounce between the positive and negative excursions due to the plus-minus asymmetries in the compliance where higher amplitude bouncing is present in the negative excursion relative to the positive excursion.

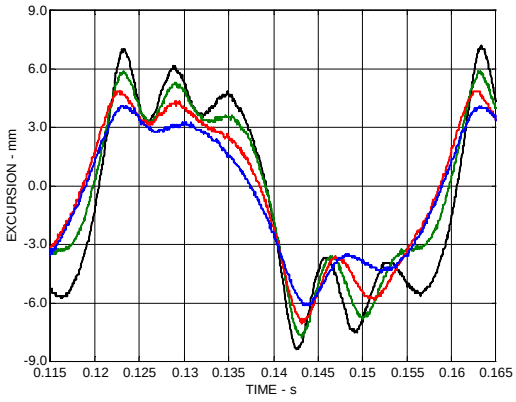

Fig. 33. Measured excursion versus time at 25 Hz. The electrical input signal was increased in 3dB steps. Large amplitude bouncing is evident at this excitation frequency on both positive and negative excursions.

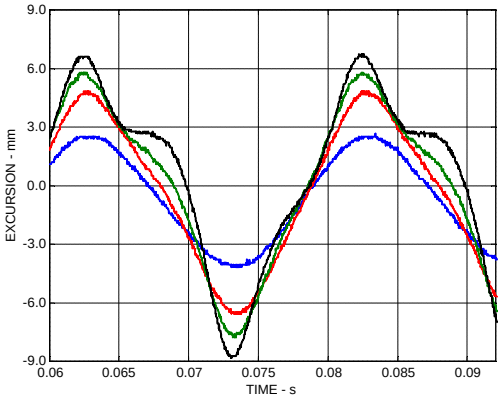

Fig. 34. Measured excursion versus time at 50 Hz. The electrical input signal was increased in 3dB steps. Bouncing is evident on both positive and negative cycles and makes itself evident as a sharpening of the waveform.

4 CONCLUSIONS

This paper has presented an alternate way of looking at the non-linear effects of a progressive loudspeaker suspension on the dynamics of its motion. The stiffness of a progressive suspension is approximately linear for excursions less than a specific value, and then rapidly increases for higher excursions. Stated another entirely equivalent way, the suspension's compliance is roughly linear for excursions below a certain value, and then quickly decreases for larger excursions.

When the loudspeaker is driven hard enough to force its excursion into the non-linear progressive part of the suspension, the suspension pushes back with much higher force. Depending on the cones velocity and kinetic energy when it enters the progressive region, this higher force can just limit the cone's maximum excursion or it can cause it to suddenly reverse direction and in effect bounce off the suspension's progressive region. This can cause sharpening of the excursion waveforms and turns sine waves into triangle waves.

If the loudspeaker's driving voltage is even higher, the high Bli force may then cause the cone to reverse direction again before it reaches the neutral excursion point ($x = 0$), thus forcing the cone outward again. This behavior can repeat itself for several cycles depending on suspension damping and cause the cone to behave somewhat like a bouncing ball.

This high-frequency bouncing behavior causes high repetitive accelerations and results in a very distorted acoustic output with very-high harmonics both in level and frequency. Cone suspension damping can be judiciously applied to minimize the effects of suspension bounce.

5 REFERENCES

[1] W. Klippel, "The Non-linear Large Signal Transfer Characteristics of Electrodynamical Loudspeakers at Low Frequencies," Preprint 3049 (H-7); 90th Convention of the Aud. Eng. Soc., February 1991.

[2] B. Zoltogorski, "Non-linear Distortions of Loudspeaker Radiators in Closed Enclosures," Preprint 4894 (F-8); 106th Convention of the Aud. Eng. Soc., May 1999.

[3] E. S. Olsen, "Nonlinear Modeling of Low Frequency Loudspeakers – A Practical Implementation," Preprint 4469 (J-4); 102nd Convention of the Aud. Eng. Soc., February 1997.

[4] E. S. Olsen & K. B. Christensen, "Nonlinear Modeling of Loudspeakers – A more complete model," Preprint 4205 (J-2); 100th Convention of the Aud. Eng. Soc., April 1996.

[5] D. Clark & R. J. Mihelich, "Modeling and Controlling Excursion Related Distortion in Loudspeakers," Preprint 4862 (A-1); 106th Convention of the Aud. Eng. Soc., April 1999.

[6] D. Clark, "Blat Distortion in Loudspeakers," Reprint 950189; Soc. Automotive Engineers Int'l Congress and Exhibition, February 1995.

[7] T. Heed, S. Iraclianos, and D. Gruenhagen, "Qualitative Analysis of Component Nonlinearities Which Cause Low Frequency THD," Preprint 4206 (J-3); 100th Convention of the Aud. Eng. Soc., May 1996.